

Supporting Information

A Novel Nanoporous Fe-doped Lithium Manganese Phosphate Material with Superior Long-term Cycling Stability for Lithium-ion Batteries

Pengjian Zuo^{*a}, Liguang Wang^a, Wei Zhang^a, Geping Yin^a, Yulin Ma^a, Chunyu Du^a,
Xinqun Cheng^a, Yunzhi Gao^a

^a School of Chemical Engineering and Technology, Harbin Institute of Technology,
No.92 West-Da Zhi Street, Harbin 150001, China

*Corresponding Author: E-mail: zuopj@hit.edu.cn, zuopjhit@gmail.com (P. Zuo)

Tel./fax: +86-451-86403216

Experimental

All chemicals are analytical grade and used without further purification. The precursor of Li_3PO_4 spheres were synthesized by a modified precipitation method¹. The 0.02 mol of H_3PO_4 was dissolved a binary solvent of 100 mL polyethylene glycol 600 (PEG600): H_2O (3: 1). Then the solution was quickly poured into another 100 mL identical binary solvent containing 0.06 mol of LiOH under strongly stirring for 20 min at room temperature. The final product was collected by filtration and washing for several times by water and ethanol, then the Li_3PO_4 was dried at 80°C for 12 h. The LMFP hollow microspheres were obtained as below: 0.025 mol of $\text{MnCl}_2\cdot 4\text{H}_2\text{O}$ and $\text{FeCl}_2\cdot 4\text{H}_2\text{O}$ (8: 2) was dissolved into 60 mL of ethylene glycol (EG) solvent in a 100 mL Teflon-lined stainless steel autoclave. Then, 0.025 mol of as-prepared Li_3PO_4 was re-dispersed into the above solution by vigorous stirring for 30 min. The autoclave was put into a preset electronic furnace and maintained at 180°C for 4 h. The obtained solution was filtered, washed with ethanol and distilled water several times and finally dried at 80°C in vacuum for 5 h. The LMFP/C was achieved by a phenolic resin solution impregnating–drying–sintering procedure. LMFP powders (0.3 g) were put into 10 mL alcohol solution contained 0.076 g phenolic resin; the slurry was magnetically stirred and dried at room temperature naturally, and then, the dried powder was sintered at 350°C for 3 h and then at 600°C for 5 h under a Ar/H_2 ($\text{Ar}:\text{H}_2 = 95:5$) atmosphere. Then the black LMFP/C powders (0.3 g) were mixed with graphene (2 mg) by an ultrasonic dispersion process to obtain the LMFP/C/G composite. Graphene was synthesized by a modified Hummers method in a two oxidation steps, as reported in

previous report.²

The X-ray powder diffraction (XRD) patterns of the products were determined by X-ray powder diffractometer (Empyrean) equipped with Cu K α radiation over the 2θ range of 10° - 90° . Morphological profiles were observed by field-emission scanning electron microscope (FESEM, FEI Helios Nanolab600i). High-resolution transmission electron microscopy (HRTEM) images were taken using a FEI Tecnai G² F30 transmission electron microscope. Fourier transform infrared (FT-IR) spectra were recorded using a Thermo Scientific Nicolet iS10 (USA) over the range of 400 - 4000 cm^{-1} with spectral resolution of 4 cm^{-1} . The amount of carbon in the composite was determined by thermogravimetric analysis (TGA) from the room temperature to 700°C at a heating rate of $10^\circ\text{C}\cdot\text{min}^{-1}$ using a Simultaneous Thermal Analysis (DSC, Netzsch STA449F3) in Ar/O₂ (Ar: 60 $\text{mL}\cdot\text{min}^{-1}$, O₂: 20 $\text{mL}\cdot\text{min}^{-1}$) atmosphere. The BET specific surface area was calculated from nitrogen adsorption isotherms using 3H-2000PS1 surface area and pore analyzer at 77K .

Electrochemical measurement was carried out by the assembly of 2025 coin-type cell with lithium metal foil as the counter and reference electrode. The slurry was obtained by mixing 80 wt% active material, acetylene black (10 wt%), and polyvinylidene fluoride (PVDF, 10 wt%) in N-methylpyrrolidone (NMP) solvent, and then coated on the aluminum foils ($\varphi=14$ mm) to form the working electrode. The mass loading in the electrode was around 2.0 $\text{mg}\cdot\text{cm}^{-2}$. 1 $\text{mol}\cdot\text{L}^{-1}$ LiPF₆ in a mixed solvent of ethylene carbonate (EC) and dimethyl carbonate (DMC) with 1:1 in volume ratio was used as the electrolyte. All cells were assembled in an Ar-filled glove box in which both

moisture and oxygen levels were less than 1 ppm. The cells were examined using a battery testing system (Neware, BST-5V3-10mA) at different charge/discharge rates between 2.5 and 4.6 V. The cells were charged at a CC-CV protocol, *i.e.*, first charged at certain current to 4.6 V followed by holding at 4.6 V for 30 min. Electrochemical impedance spectra (frequency range: 0.01-10⁵ HZ) of electrodes in coin-type cells after three cycles were performed with an electrochemical workstation (PARSTAT 2273).

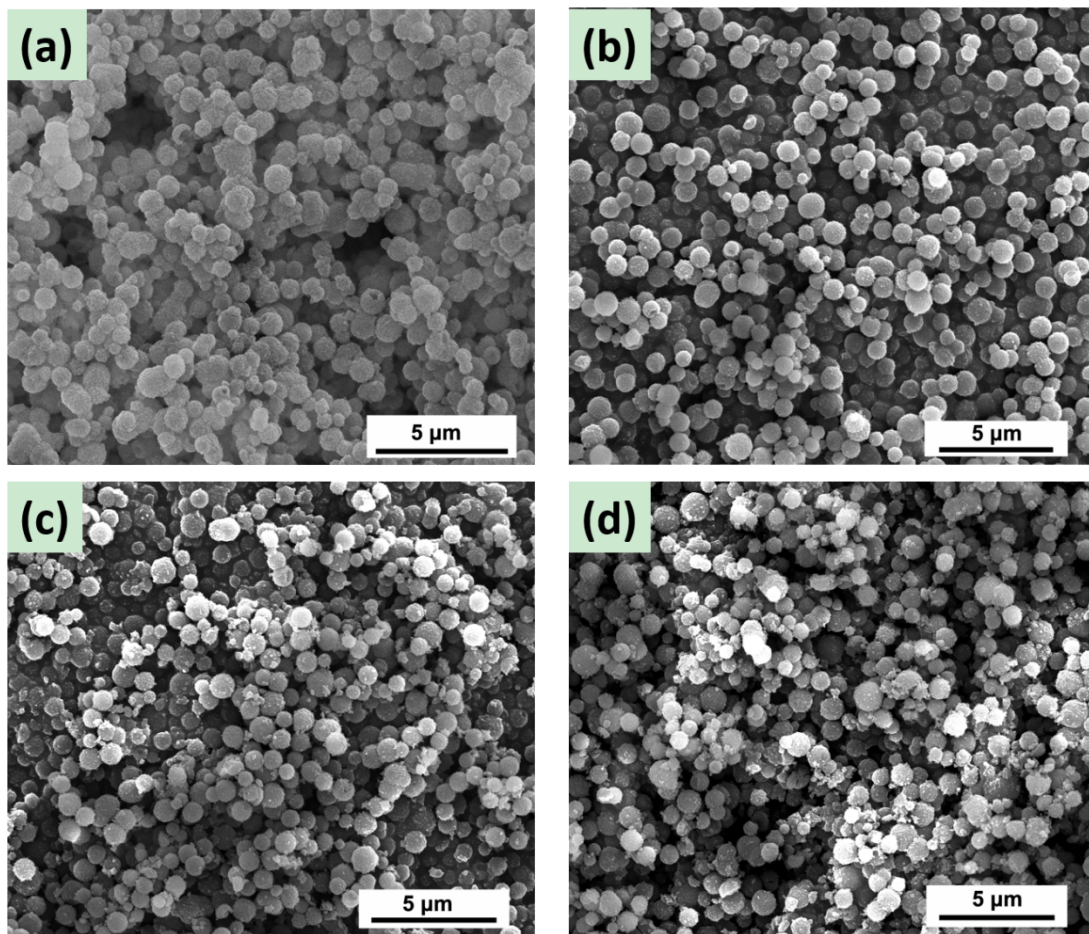


Figure S1. SEM images of Li_3PO_4 obtained under different pH value: (a) 10.5; (b) 11.0; (c) 11.5; (d) 12.0.

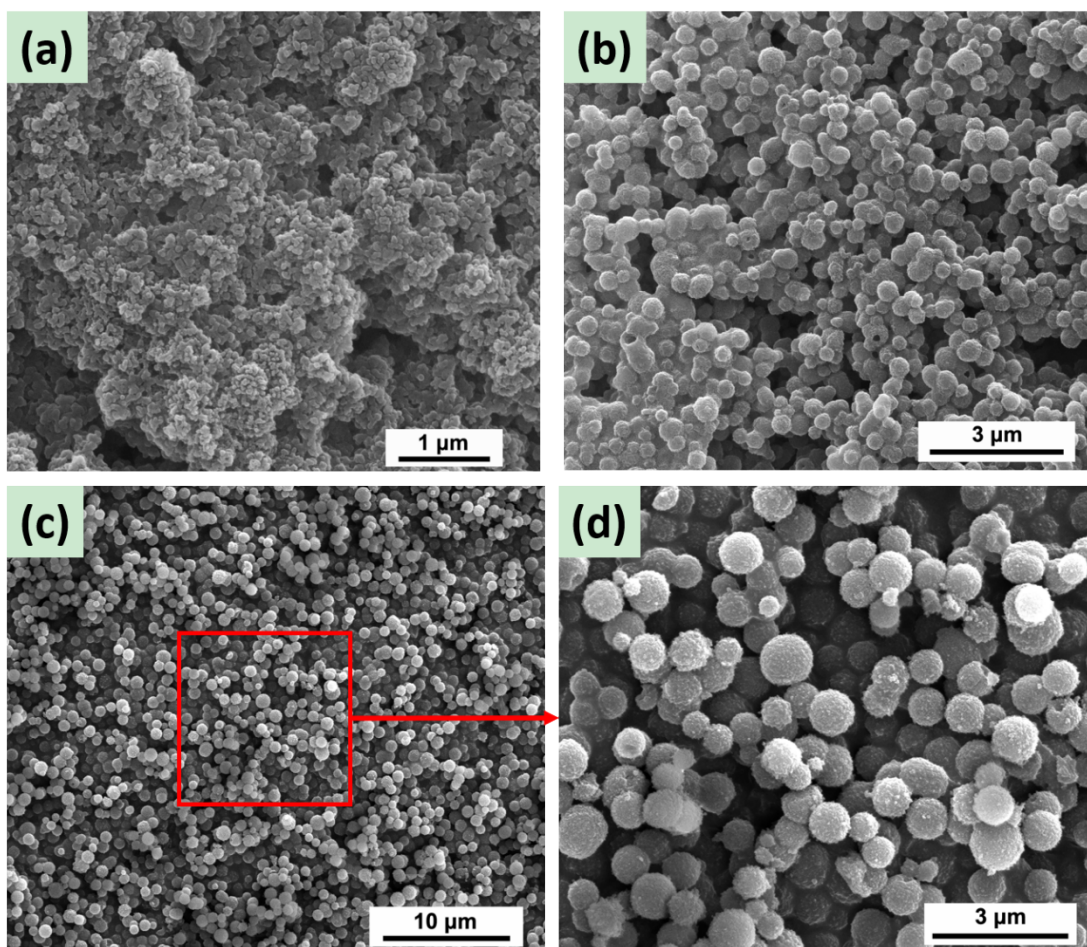


Figure S2. SEM images of Li_3PO_4 obtained by different time: (a) 0 min; (b) 10 min; (c, d) 20 min.

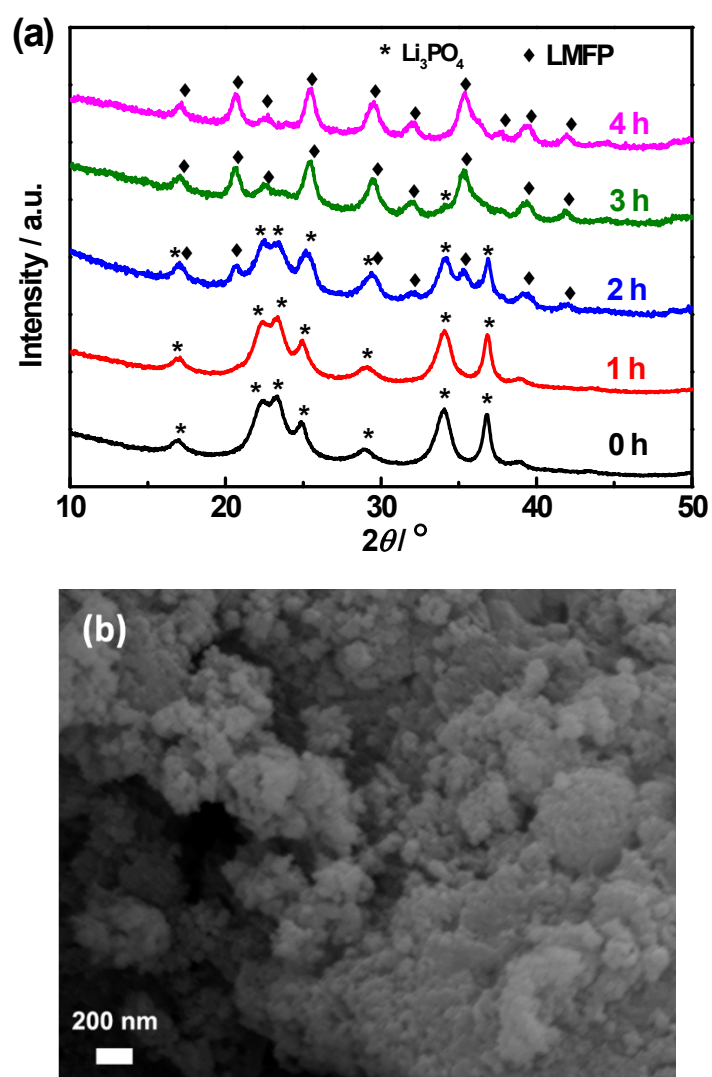


Figure S3. (a) XRD patterns show the phase transformation from Li_3PO_4 to LMFP.

The samples were collected after solvothermal treatment at 180°C for different times:

0 h-4 h. (b) SEM image of nano-LMFP/C/G.

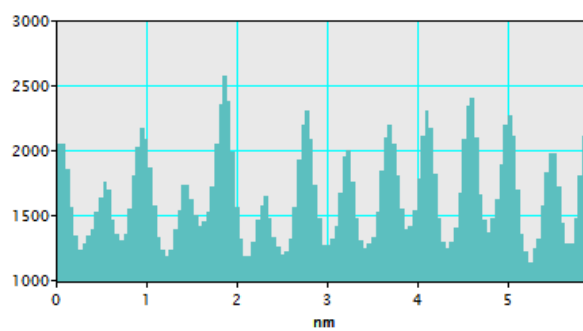


Figure S4. The intensity maps of HRTEM image (Figure 2e) along yellow line.

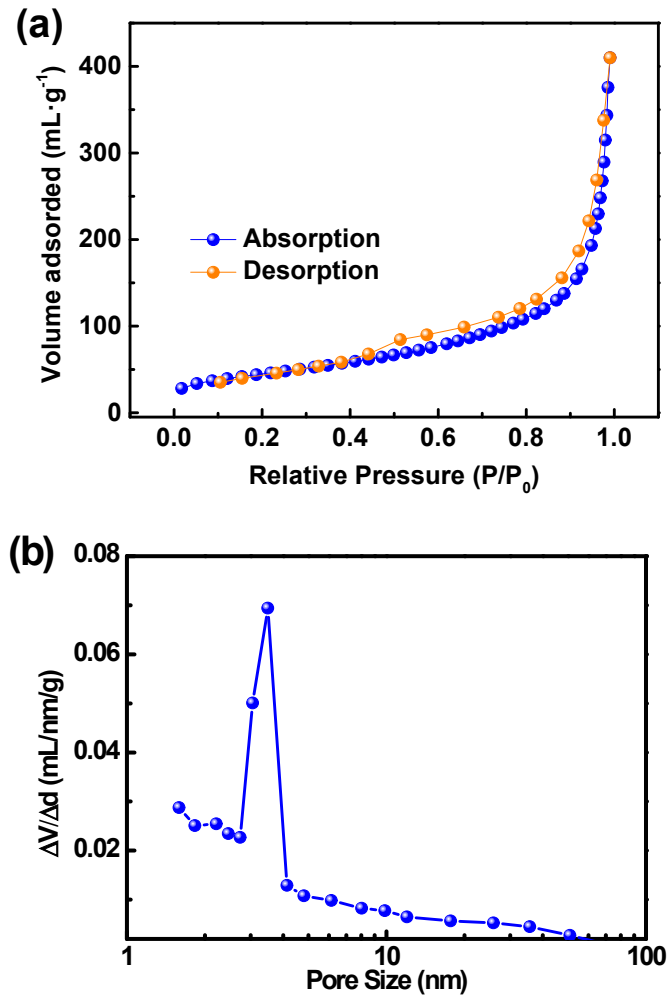


Figure S5. (a) Nitrogen sorption isotherm and (b) pore size distribution of nano-LMFP/C/G.

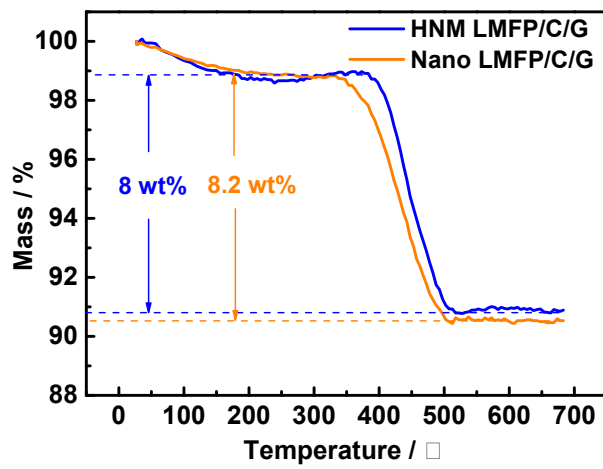


Figure S6. TG curves of HNM-LMFP/C/G and Nano-LMFP/C/G.

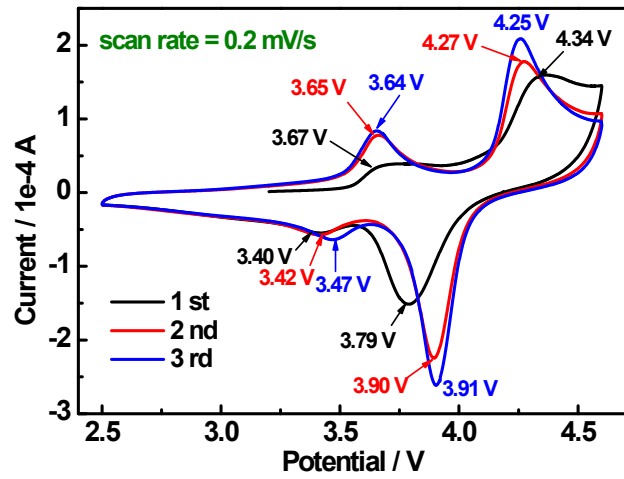


Figure S7. The first three cycles cyclic voltammetry (CV) curves of HNM-LMFP/C/G at the scan rate of $0.2 \text{ mV} \cdot \text{s}^{-1}$.

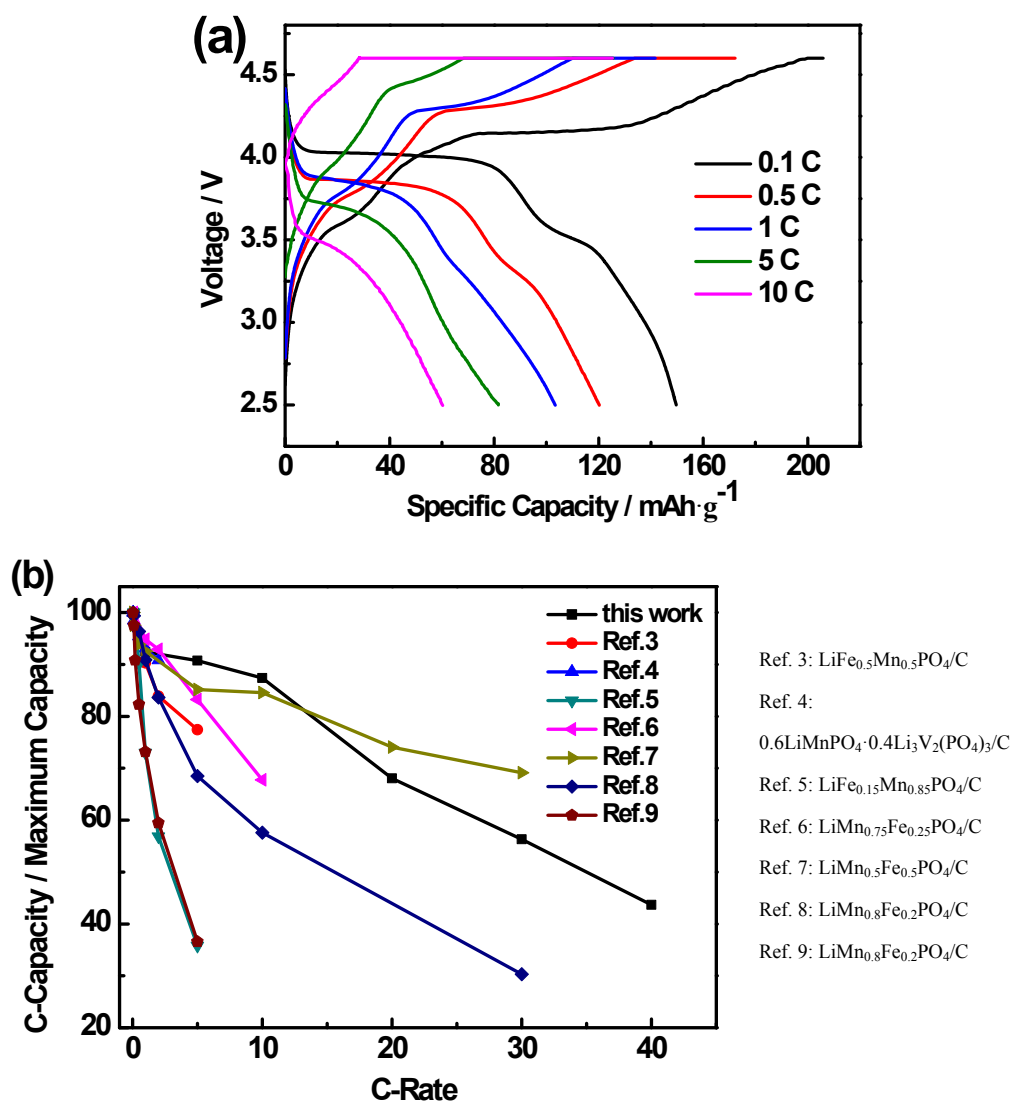


Figure S8. (a) Initial charge/discharge curves of nano-LMFP/C/G. (b) Comparison of rate performance with other research group.³⁻⁹

From the comparison of rate performance with other research group, we can see that the rate performance of the HNM-LMFP/C/G is better than the most of lithium manganese phosphate materials reported in the previous paper. However, the $\text{LiMn}_{0.5}\text{Fe}_{0.5}\text{PO}_4/\text{C}$ composite in Ref. 7 has the better rate performance than that of this work, which would contribute to the more Fe^{2+} doping. Because the more Fe^{2+} ions in the LiMnPO_4 crystal, the material has the better rate performance as have been proved.¹⁰

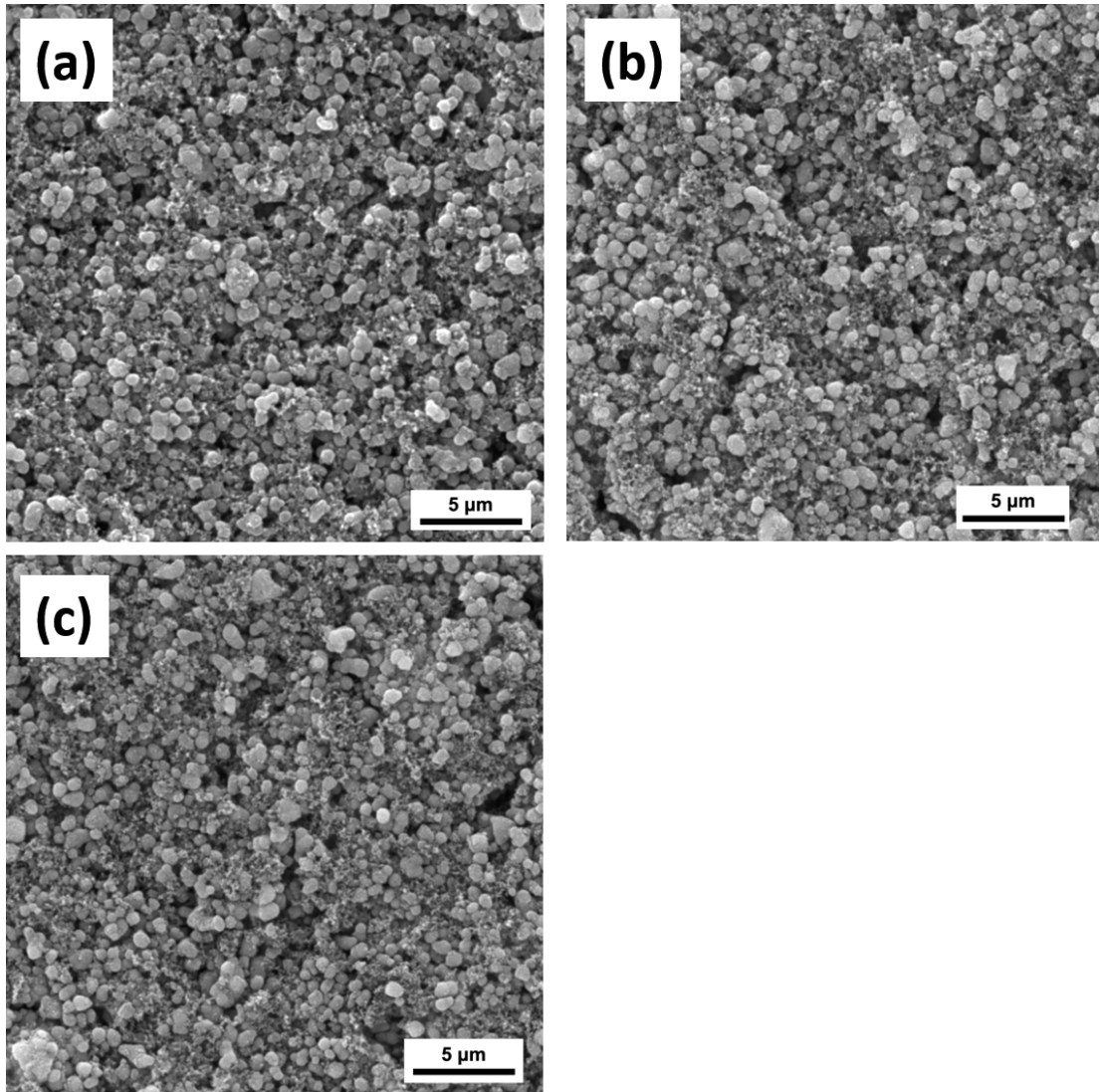


Figure S9. The SEM images of the HNM-LMFP/C/G electrode (a) without cycling, (b) after 500 cycles and (c) 900 cycles at 10 C.

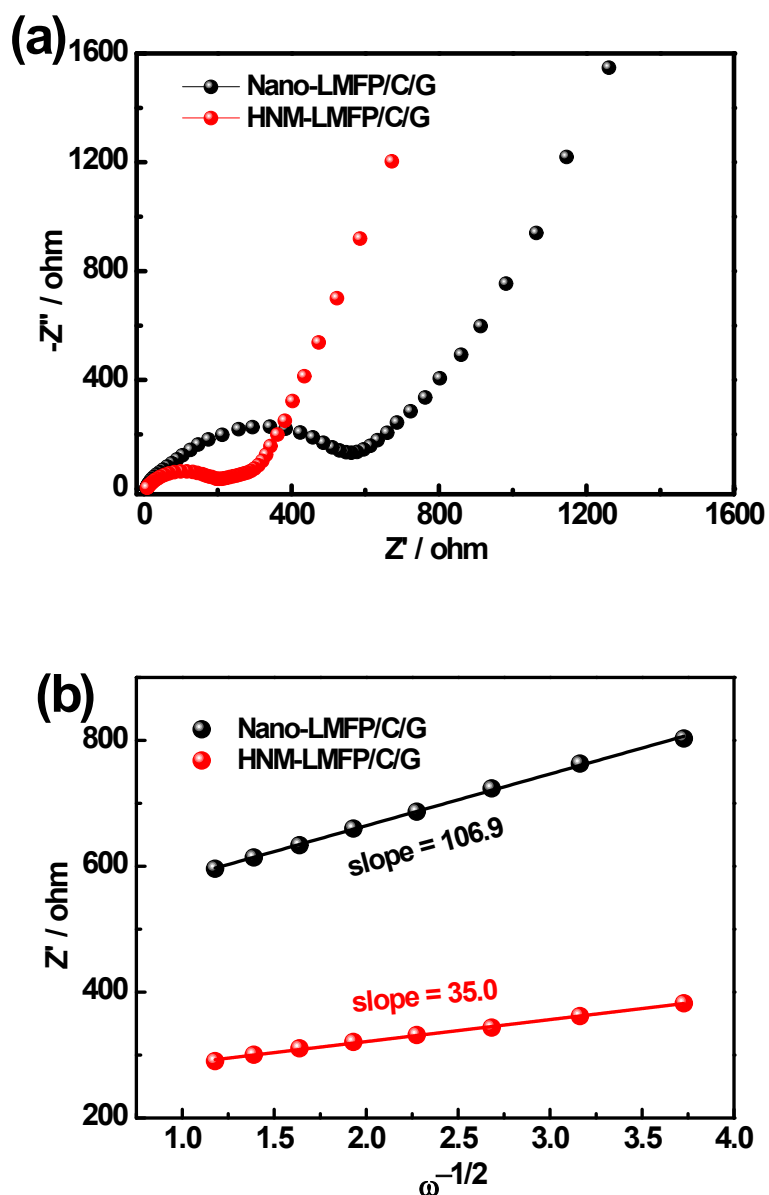


Figure S10. (a) Nyquist plots (Z' vs. $-Z''$) of the samples; (b) the relationship plot of Z' vs. $\omega^{-1/2}$ at low-frequency region.

Reference

1. S.-L. Yang, R.-G. Ma, M.-J. Hu, L.-J. Xi, Z.-G. Lu and C. Y. Chung, *J. Mater. Chem.*, 2012, **22**, 25402.
2. Z. Yongguang, Z. Yan, A. Vermukhambetova, Z. Bakenov and P. Chen, *J. Mater. Chem. A*, 2014, **1**, 295.
3. X. Zhou, Y. Xie, Y. Deng, X. Qin and G. Chen, *J. Mater. Chem. A*, 2015, **3**, 996.
4. C. Wang, Y. Bi, Y. Liu, Y. Qin, Y. Fang and D. Wang, *J. Power Sources*, 2014,

263, 332.

5. X. Zhou, Y. Deng, L. Wan, X. Qin and G. Chen, *J. Power Sources*, 2014, **265**, 223.
6. M.-S. Kim, J.-P. Jegal, K. C. Roh and K.-B. Kim, *J. Mater. Chem. A*, 2014, **2**, 10607.
7. Z.-X. Chi, W. Zhang, X.-S. Wang, F.-Q. Cheng, J.-T. Chen, A.-M. Cao and L.-J. Wan, *J. Mater. Chem. A*, 2014, **2**, 17359.
8. S. K. Martha, J. Grinblat, O. Haik, E. Zinigrad, T. Drezen, J. H. Miners, I. Exnar, A. Kay, B. Markovsky and D. Aurbach, *Angew. Chem. Int. Ed.*, 2009, **48**, 8559.
9. Y. Hong, Z. Tang, Z. Hong and Z. Zhang, *J. Power Sources*, 2014, **248**, 655.
10. H. Wang, Y. Yang, Y. Liang, L. Cui, H. S. Casalongue, Y. Li, G. Hong, Y. Cui and H. Dai, *Angew. Chem.*, 2011, **123**, 7502.